$A_5TaAs_4Tl_2$ (A = Rb, K). Transition-Metal Zintl Phases with a Novel Complex Ion: Synthesis, Structure, and Bonding

DaPing Huang and John D. Corbett*

Ames Laboratory−DOE[1] and Department of Chemistry, Iowa State University, Ames, Iowa 50011

Received March 5, 1998

Reactions of the Rb−Tl−As system near 500 °C in tantalum containers always lead to the formation of $Rb_5TaAs_4Tl_2$ because of reactions with the container wall. On-stoichiometry reactions of these three elements in Ta, or of the four components in SiO_2, afford the pure compound. $Rb_5TaAs_4Tl_2$ crystallizes in orthorhombic system, space group *Pnma* (No. 62), $Z = 4$, $a = 19.196(5)$ Å, $b = 11.104(3)$ Å, $c = 7.894(4)$ Å. The isostructural $K_5TaAs_4Tl_2$ also exists. The main structural feature is the closed-shell polyanion $TaAs_4Tl_2^{5-}$ which can be viewed as the result of a reaction of a $TaAs_4^{7-}$ tetrahedron with two Tl^+ so as to bridge opposed edges of the former. EHMO calculations for $TaAs_4^{7-}$ (T_d) and $TaAs_4Tl_2^{5-}$ (D_{2h}) demonstrate the character of the bonding of Tl s and p to the electron-rich As. Two kinds of multicentered bonds are evident: $\pi_\perp$ and σ plus $\pi_\parallel$ in the plane of the $TlAs_2Ta$ portions and 5c−4e $d-p$ bonds within $TaAs_4$.

Introduction

Thallium has turned out to be extremely prolific in the formation of alkali-metal compounds that contain a variety of novel thallium clusters Tl_n^{m-} ($3 \le n \le 13$) or networks of clusters, or both.[2−7] Both self- and heterometal-centered clusters are found, and some among these are examples of hypoelectronic behavior relative to the expectations of Wade's rules. The present compound resulted from an effort to obtain heteroatomic cluster anions through introduction of the pnictogen arsenic into the Rb−Tl compounds, following our investigations of some mixed Tl−Sn anionic systems.[8] This led instead to the unanticipated oxidation of the Ta container and to the production of the unusual $Rb_5TaAs_4Tl_2$.

None of the 12 known phases that contain both arsenic and thallium (according to Pearson[9]) contains any As−Tl bonds. However, related tetrahedral metal arsenide anions TAs_4^{7-} for T = Nb, Ta have been isolated as the salts A_7TAs_4, A = Rb, K.[10] These are classical valence compounds that can also be described as transition-metal Zintl phases,[11] analogous to the main-group A_8SiAs_4 (A = alkali metal)[12] and so forth. (However, it is not very likely that strictly isostructural A_7PnAs_4 main-group analogues of A_7TaAs_4 can be obtained by normal synthetic routes for Pn = Sb, Bi, etc. because of the disparity in oxidation states.) The $(TaAs_4)Tl_2^{5-}$ unit reported in the present article is novel because it can be thought of as arising from the secondary coordination of Tl^+ to bidentate $TaAs_4^{7-}$ units. This process will be considered theoretically in the same way. We will continue to write the formula for the compound and the anion as $TaAs_4Tl_2$ in order to emphasize the connectivity.

Experimental Section

Synthesis. The general reaction techniques in welded Ta tubing have been described elsewhere.[2−6] All operations were carried out in N_2- or He-filled gloveboxes because of the sensitivity of both the alkali metals and the products to air and moisture. Before use, the Tl (99.998%, Johnson-Matthey), K (99.9%, Baker), and Rb (99.9%, Johnson-Matthey) metals utilized were cleaned with a scalpel, and As (99.998%, Johnson-Matthey) was ground into powder.

$Rb_5TaAs_4Tl_2$ was the first seen in good yield following a reaction of the elements in the proportions $Rb_4As_4Tl_2$ that had been run in welded Ta tubing. This had in turn been sealed into an evacuated silica jacket and heated to 500 °C for 1 day, followed by cooling to room temperature at 2 °C/h. Many black plate-like crystals were found sticking to the inner wall of Ta tubing, which had visibly reacted. The same product was obtained from a $Rb_6As_2Tl_2$ composition according to the product's Guinier powder pattern to which Si had been added as an internal standard. Reaction with a 2:2:6 molar ratio of Rb/As/Tl heated instead to 700 °C for 2 days and similarly cooled also yielded the title phase, in part.

These results at first suggested that As might have been preferentially more reactive with Ta than with Rb as a number of binary Ta−As compounds are known.[13] However, a revised reaction strategy showed that the new compound is thermodynamically stable with respect to other possibilities or, in other words, that an $Rb_5As_4Tl_2$ composition is quite oxidizing to Ta. The title phase was also obtained from reactions

(1) This research was supported by the Office of the Basic Energy Sciences, Materials Sciences Division, U.S. Department of Energy. The Ames Laboratory is operated for DOE by Iowa State University under Contract No. W-7405-Eng-82.
(2) Dong Z.-C.; Corbett, J. D. *J. Am. Chem. Soc.* **1994**, *116*, 3429.
(3) Dong Z.-C.; Corbett, J. D. *J. Am. Chem. Soc.* **1995**, *117*, 6447.
(4) Dong Z.-C.; Corbett, J. D. *Inorg. Chem.* **1996**, *35*, 1444.
(5) Dong Z.-C.; Corbett, J. D. *Angew. Chem., Int. Ed. Engl.* **1996**, *35*, 1006.
(6) Dong Z.-C.; Corbett, J. D. *Inorg. Chem.* **1996**, *35*, 2301.
(7) Corbett, J. D. In *Chemistry, Structure, and Bonding of Zintl Phases and Ions*; Kauzlarich, S. M., Ed.; VCH Publishers: New York, 1996; Chapter 3.
(8) Huang, D.-P.; Corbett, J. D. Unpublished research.
(9) Villars, P.; Calvert, L. D. *Pearson's Handbook of Crystallographic Data for Intermetallic Phases*, 2nd ed.; American Society for Metals International: Metals Park, OH, 1991.
(10) Nuss, J.; Cordoso Gil, R. H.; Hönle, W.; Peters, K.; von Schering, H.-G. *Z. Anorg. Allg. Chem.* **1996**, *622*, 1854.
(11) Kauzlarich, S. M. In *Chemistry, Structure, and Bonding of Zintl Phases and Ions*; Kauzlarich, S. M., Ed.; VCH Publishers: New York, 1996; Chapter 6.
(12) von Schnering, H.-G.; Hartweg, M.; Kalpen, H.; Nuss, J.; Hönle, W. *Z. Kristallogr.* **1988**, *182*, 239.
(13) *Binary Alloy Phase Diagrams*, 2nd ed.; Massalski, T. B., Ed.; ASM International: Materials Park, OH, 1990; Vol. 3, p 2734.

S0020-1669(98)00239-0 CCC: $15.00
Published on Web 07/24/1998

Table 1. Some Data Collection and Refinement Parameters for $Rb_5TaAs_4Tl_2$

fw	1316.7
cryst syst	orthorhombic
space group, Z	*Pnma* (No. 62), 4
lattice constants (Å)[a]	$a = 19.200(5)$
	$b = 11.123(5)$
	$c = 7.824(4)$
volume (Å^3)	1683(2)
temperature (°C)	23‘
d_c (g/cm^3)	5.195
μ, cm^{-1} (Mo Kα)	474.36
R/R_w[b] (%)	4.4/4.9

[a] Guinier powder pattern data, $\lambda = 1.540\,562$ Å, 23 °C. [b] $R = \sum||F_o| - |F_c||/\sum|F_o|$; $R_w = (\sum w(|F_o| - |F_c|)^2/\sum w|F_o|^2)^{1/2}$; $w = \sigma_F^{-2}$.

of RbAs and Rb_3As (also prepared from the elements in Ta at 400 °C) with Ta powder and Tl chunks so as to afford $Rb_7TaAs_4Tl_2$ compositions. Portions of this mixture were separately sealed into both Ta and SiO_2 containers, heated at 700 °C for 3 days, and slowly cooled at 1 °C/h. Both products were evidently single phase according to the Guinier powder patterns (where free Rb is not easily detected) and contained no Ta metal lines. Similarly, samples of composition 5:1:4:2 and 5:0:4:2 run in Ta under the first conditions described above both gave the pure compound according to their powder patterns. EDS (energy dispersive spectroscopy) measurements on these two products on a JEOL JSM-830 instrument gave Rb/Ta/Tl/As proportions (at %) of 46:7:14:33 and 46:8:12:36, with uncertainties up to about ±2% in each element, vs the ideal 41.7:8.3:16.7:33.3. The Ta value in the second reaction clearly came from oxidation of the Ta tubing.

A powder pattern taken after a similar reaction loaded with potassium instead showed that the isostructural $K_5TaAs_4Tl_2$ exists: $a = 18.458(7)$ Å, $b = 10.680(6)$ Å, $c = 7.588(5)$ Å.

Structure Determination. A black platelike crystal about 0.30 × 0.20 × 0.03 mm was selected from first reaction, sealed in a thin-walled capillary, and checked by Laue photographs for its singularity and quality. Data were collected on a Rigaku AFC6R diffractometer at 23 °C using graphite-monochromated Mo Kα radiation. The 25 reflections from a random search covering $14 \le 2\theta \le 20°$ yielded an orthorhombic cell: $a = 19.196(5)$ Å, $b = 11.104(3)$ Å, and $c = 7.834(4)$ Å. The Laue check indicated an *mmm* class. Two octants of data were collected over the region of $3 \le 2\theta \le 55°$. The diffraction data were corrected for absorption with the aid of three ψ scans of strong reflections. Space group *Pnma* (No. 62) was chosen on the basis of the intensity analysis, which indicated a centric space group, and the systematic absences *0kl* ($k + l \neq 2n$ and *hk*0 ($h \neq 2n$). The intensities of three standard reflections checked every 150 reflections showed no significant decay.

The structure was solved by direct methods employing SHELXS[14] and refined using the TEXSAN package.[15] All atoms were correctly located in the SHELXS output. Since the aspect ratio of the crystal was large (~10:1) and the absorption was severe (474 cm^{-1}), the ψ scan absorption correction was not sufficient. The semiempirical absorption correction DIFABS[16] was applied to correct the data better after isotropic refinement had converged at $R(F)/R_w = 0.081/0.085$, GOF = 4.14. Isotropic refinement then yielded $R(F)/R_w = 0.060/0.064$, with notably smaller positional errors, and the individual ellipsoids became distinctly more uniform and precise as well in the converged anisotropic refinement, $R(F) = 0.044$, $R_w = 0.049$, GOF = 1.74. The largest residual peaks were 2.33 and −2.13 e/Å^3 at 0.2344, 1/4, 0.5122 and 0.1660, 1/4, 0.7430, respectively, about 1.4 and 1.2 Å from the Ta atom. A distinctive ellipsoid for Rb3, with an aspect ratio of 3:1 along $\vec{z}$ arises because of its very flattened coordination polyhedron of two Tl, two Rb, and three As atoms, all at ≤3.95 Å.

Some data collection and refinement parameters are listed in Table 1. The atomic positions plus isotropic equivalent displacement parameters and the closer interatomic distances are given in Tables 2 and 3, respectively. More data collection and refinement details and the anisotropic displacement parameters are available in the Supporting Information, and these plus the F_o/F_c listing are also available from J.D.C.

Table 2. Positional and Isotropic Displacement Parameters for $Rb_5TaAs_4Tl_2$

atom[a]	x	y	z	B_{eq}[b]
Tl1	0.0541(1)	1/4	0.9146(4)	2.2(1)
Tl2	0.3120(1)	1/4	0.3271(3)	2.2(1)
Ta1	0.1638(1)	1/4	0.5841(4)	1.3(1)
As1	0.1018(2)	0.0690(5)	0.6966(6)	2.0(2)
As2	0.1637(4)	1/4	0.2691(8)	2.0(3)
As3	0.2903(3)	1/4	0.6698(9)	1.6(3)
Rb1	0.2485(2)	0.0539(5)	0.9804(5)	2.3(2)
Rb2	−0.0234(4)	1/4	0.392(1)	4.0(4)
Rb3	0.0780(2)	0.5249(5)	0.1917(8)	3.8(3)

[a] All positions are 8*d* or 4*c* (*m*). [b] $B_{eq} = (8\pi^2/3)\sum_i\sum_j U_{ij}\boldsymbol{a}_i^*\boldsymbol{a}_j^*\boldsymbol{a}_i\boldsymbol{a}_j$.

Table 3. Selected Bond Distances (Å) and Angles (deg) in $Rb_5TaAs_4Tl_2$

Tl1−Ta1	3.354(4)		
Tl1−As1	2.801(5) 2×	As3−Ta1	2.521(7)
Tl1−As2	3.502(7)	As3−Tl2	2.739(7)
Tl1−Rb3	3.783(6) 2×	As3−Rb1	3.377(7) 2×
Tl1−Rb3	3.658(6) 2×	As3−Rb1	3.766(6) 2×
		As3−Rb3	3.560(7) 2×
Tl2−Ta1	3.495(4)		
Tl2−As2	2.883(8)	Rb1−Ta1	3.858(5)
Tl2−As3	2.739(7)	Rb1−Tl2	3.705(5)
Tl2−Rb1	3.705(5) 2×	Rb1−Tl2	3.769(5)
Tl2−Rb1	3.769(5) 2×	Rb1−As1	3.603(7)
Tl2−Rb2	3.601(8)	Rb1−As1	3.609(7)
		Rb1−As2	3.548(7)
Ta1−As1	2.499(5) 2×	Rb1−As3	3.377(7)
Ta1−As2	2.488(7)	Rb1−As3	3.766(7)
Ta1−As3	2.521(7)	Rb1−Rb3	3.778(7)
Ta1−Rb1	3.858(5) 2×		
Ta1−Rb2	3.902(9)	Rb2−Ta1	3.902(8)
		Rb2−Tl2	3.601(8)
As1−Ta1	2.499(5)	Rb2−As1	3.952(8) 2×
As1−Tl1	2.801(5)	Rb2−As1	3.912(6) 2×
As1−Rb1	3.603(7)	Rb2−As2	3.72(1)
As1−Rb1	3.609(7)	Rb2−Rb3	3.950(7) 2×
As1−Rb2	3.912(6)		
As1−Rb2	3.952(8)	Rb3−Tl1	3.783(6)
As1−Rb3	3.596(7)	RRb3−Tl1	3.658(6)
		Rb3−As1	3.596(7)
As2−Ta1	2.488(7)	Rb3−As2	3.522(6)
As2−Tl2	2.883(8)	Rb3−As3	3.560(7)
As2−Rb1	3.548(7) 2×	Rb3−Rb1	3.778(7)
As2−Rb2	3.72(1)	Rb3−Rb2	3.950(7)
As2−Rb3	3.522(6)		

As1−Tl1−As1	91.7(2)	As1−Ta−As1	107.1(7)
As2−Tl2−As3	90.4(2)	As2−Ta−As3	105.6(3)
Ta−As1−Tl1	78.3(2)	As1−Ta−As3	111.3(2)
Ta−As2−Tl2	80.8(2)	As1−Ta−As2	110.8(2)
Ta−As3−Ta2	83.2(2)		

Calculations. The EHMO investigations carried out for bonding investigations employed the suite of programs developed by R. Hoffmann and co-workers at Cornell University. The orbital exponents were default values, while the energy parameters came from density functional theory calculations.[17]

Results and Discussion

Structure. The structure of the isolated $TaAs_4Tl_2^{5-}$ anion is illustrated in Figure 1. This is easily seen to result from bridging of the trans edges of a classical $TaAs_4^{7-}$ tetrahedron by two Tl^+ atoms, the σ bonding to each Tl arising with electron

(14) Sheldrick, G. M. *SHELXS-86*; Universität Göttingen: Germany, 1986.
(15) *TEXSAN*, Version 6.0; Molecular Structure Corp.: The Woodlands, TX, 1990.
(16) Walker, N.; Stuart, D. *Acta Crystallogr.* **1983**, *A39*, 158.
(17) Vela, A.; Gázquez, J. L. *J. Phys. Chem.* **1988**, *92*, 5688.

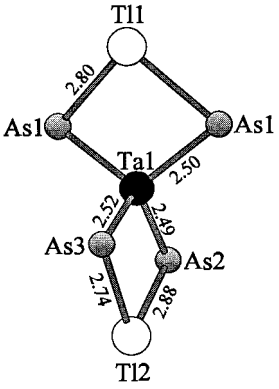

Figure 1. Structure of and distances within the $[TaAs_4Tl_2]^{5-}$ anion in $Rb_5TaAs_4Tl_2$.

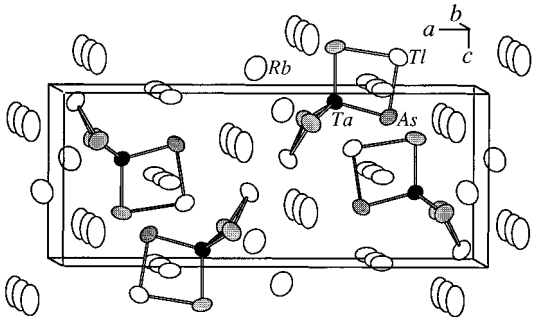

Figure 2. [010] projection of the unit cell $Rb_5TaAs_4Tl_2$ (*Pnma*) (90% probability ellipsoids).

pairs on the two arsenic atoms. One could then imagine, and theory shows it to be correct, that the remainder of the octet at thallium comes from a π-bonding system centered on Tl.

The arrangement of the ions in the solid compound is shown in a [010] projection of the unit cell in Figure 2. The Ta, both Tl, and the As2, As3 atoms all lie in a mirror plane at $y = {}^1/_4$ and ${}^3/_4$, accounting for the distribution of independent distances shown in Figure 1. A slightly uneven distribution of d(Tl−As) distances, 2.8015(5) (×2), 2.883(8) and 2.739(7) Å, is found for Tl1−As1, Tl2−As2, and Tl2−As3, respectively, with $\bar{d} =$ 2.81 Å. There are no prior examples of Tl−As bonds. While the sum of the tetrahedral covalent radii according to Pauling[18] is 2.65 Å, the utility of the Tl value therein seems questionable since it was derived from tetrahedral Tl surroundings in a pyrite-like structure, namely as $[d(\text{Tl−S}) - {}^1/_2 d(\text{S−S})]$.[19] A better agreement, 2.80 Å, is obtained if one-half of d(Tl−Tl) in the diamond network in NaTl[20] is used for the metal instead, but this may in turn suffer from mixing of different sets of radii.

The configuration about the Ta atom is roughly tetrahedral and $\bar{d}$(Ta−As), 2.502(6) Å, is just 0.011(6)Å less than that reported in Rb_7TaAs_4.[10] The individual Ta−As distances show a range of 0.033(10) Å. The bridging Tl atoms elongate the tetrahedron slightly in an angular sense, decreasing the internal As−Ta−As angles to 107 and 106° at Tl1 and Tl2, respectively. The angles at Tl, 91.7(2) and 90.4(2)°, are consistent with their dominant p-orbital bonding while the angles at As give way the most, 78° to 83°. A small fold of the Ta−As1−Tl1 portion at As···As is evident in Figure 2 as well, such that the dihedral angle between As1−Tl1−As1 and As1−Ta−As1 is 25.3°. This presumably arises from packing. The other ring is planar

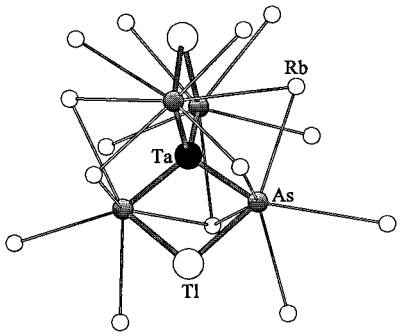

Figure 3. Cation environment of the $[TaAs_4Tl_2]^{5-}$ anion. The limits for the marked separations are 4.0 Å for Tl−Rb and As−Rb and 3.9 Å for Ta−Rb.

according to the mirror plane, and, of course, so is the symmetry of its surroundings. There are no disparate displacements of the heavy atoms from this plane among the thermal ellipsoid data either.

The distribution of Rb^+ about the anion, particularly with regard to As neighbors, is illustrated in Figure 3. The arsenic atoms have five to six Rb^+ neighbors over a rather large distance range, 3.38−3.95 Å, and most of the bridging functions are irregular. The thallium atoms clearly prohibit some cations from coming close to As; As−Rb coordination numbers of 10 occur in Rb_7TaAs_4.

Bonding. The classification of transition-metal *Zintl* phases is an unfinished problem, because the *d* orbitals of these metals are traditionally allowed to be partly filled according to the more open-ended definition of this type of compound.[11] Only some compounds that contain late transition metals (e.g., from the Zn and Cu families) may be reasonably viewed as having filled d shells. The present compound falls at the other end of the spectrum, as tantalum is formally d^0.

EHMO calculations have been carried out sequentially in order to assist the description of the bonding change from $TaAs_4^{7-}$ (T_d) to $TaAs_4Tl_2^{5-}$ (D_{2d}), using in each case the average bond lengths for the rubidium salt. The MO diagram for $TaAs_4^{7-}$ is illustrated in Figure 4. For convenience, the s orbitals of the arsenic atoms are omitted from the plot since their energies are low (<-19 eV), although the overlap populations between these ($1a_1$ and $1t_2$) and thallium s and p in the ternary ion are significant (below). The pair of lower lying $2t_2$ and $3t_2$ orbital sets in Figure 4 are primarily π and σ (the higher) according to the As-based linear combinations. These two MOs turn out to lie at somewhat higher energies than the π-bonding 1e MO. The σ-bonding $2a_1$ MO comes from the Ta s and As p while the t_1 states lie only on the As ligands. Therefore, four mainly σ bonds and two plus three π bonds pertain to $TaAs_4^{7-}$ anion, as is usual for transition-metal TX_4 tetrahedra.[21] The π-bonding splitting (e, e*) is only a little less than that of the σ $3t_2$, $4t_2$* because of the geometry and relative energies.

The bonding scheme for the formation of the $TaAs_4Tl_2^{5-}$ anion from $TaAs_4$ and two Tl is shown over a wider energy range in Figure 5, while the overlap populations (OP) for the new Tl−As bonds are summarized in Table 4. The degenerate orbitals of the $TaAs_4$ tetrahedral anion are all split owing to the reduction of symmetry from T_d to D_{2d} on bonding Tl to As. Some large splittings stem from strong σ interactions of the 1e and $2t_2$ orbitals of $TaAs_4^{7-}$ with Tl s, the interactions leading to two bonding orbitals, $2a_1$ and $2b_2$, and the roughly nonbond-

(18) Pauling, L. *The Nature of the Chemical Bond*; Cornell University Press: Ithaca, NY 1960; p 246.
(19) Pauling, L.; Huggins, M. L. *Z. Kristallogr.* **1934**, *87*, 205.
(20) Schmidt, P. C.; Baden, W.; Weiden, N.; Weiss, A. *Phys. Status Solidi* **1985**, *92A*, 205.
(21) Carter, R. L. *Molecular Symmetry and Group Theory*; Wiley: New York, 1998; p 226.

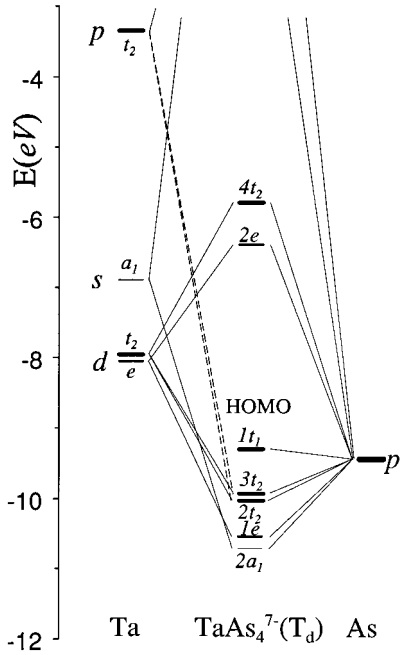

Figure 4. Molecular orbital diagram for the tetrahedral $TaAs_4^{7-}$ anion, showing the splitting of a, e, and t_2 orbitals. Degeneracies are represented by thicker lines. The low-lying s orbitals of the As atoms (<-19 eV) are not plotted.

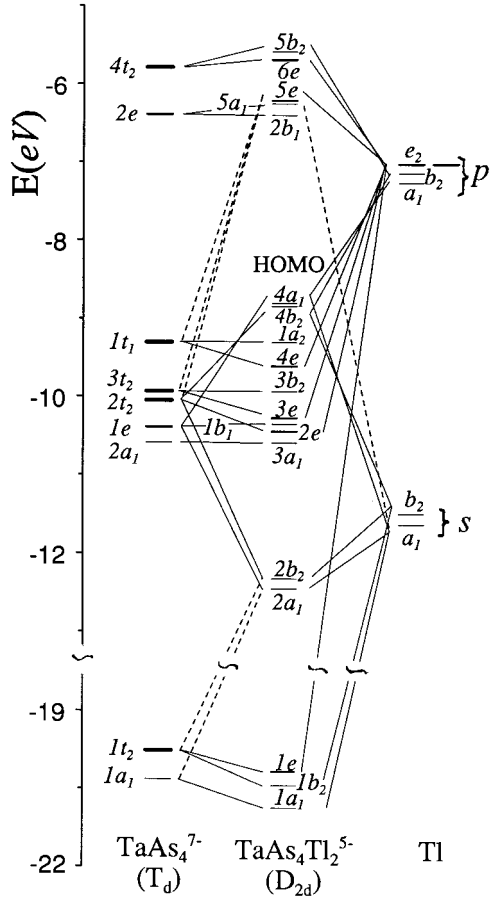

Figure 5. MO scheme for the $(TaAs_4Tl_2)^{5-}$ anion from $TaAs_4^{7-} + 2Tl^+$.

ing $4b_2$ and $4a_1$ (which involve Tl p as well). Since electrons in $TaAs_4Tl_2^{5-}$ fill up through the $4a_1$ HOMO, the last two ostensibly counteract the first pair in Tl s contributions, but not entirely so when Tl p mixing in the latter is included (Table 4).

Table 4. Tl−As Bond Types in $TaAs_4Tl_2^{5-}$ and Their Overlap Populations[a]

MO	σ_{s-s}	σ_{p-s}	σ_{s-p}	σ_{p-p}	$\pi(\perp)^b$	$\pi(\parallel)^c$
$1a_1$	0.025	0.039				
$1b_2$	0.028	0.045				
1e		0.106				
$2a_1$	−0.020	0.005	0.112	−0.015		
$2b_2$	−0.025	0.006	0.122	−0.014		
$3a_1$						−0.006
2e		−0.007		0.071	0.029	0.041
$1b_1$						
3e					0.069	0.022
$3b_2$						
4e		−0.012	0.062		0.020	−0.016
$1a_2$						
$4b_2$			−0.088	0.082		
$4a_1$			−0.080	0.060		−0.006
total OP	0.011	0.183	0.065	0.236	0.118	0.039

[a] Per atom pair. Overlap populations (OP) less than ±0.005 are not listed but are included in the totals. [b] $\pi(\perp)$ is for p orbitals perpendicular to the $TlAs_2$ plane. [c] $\pi(\parallel)$ is the π component of p orbitals lying in the $TlAs_2$ plane.

Chart 1

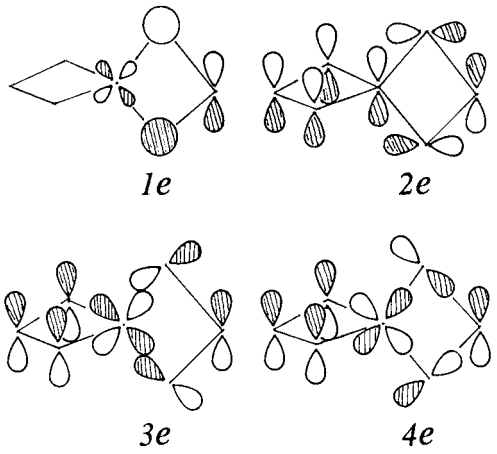

The bonding 2e split from the above $2t_2$ as well as 3e and 4e from $3t_2$ and $1t_1$ on the tetrahedron all originate from interactions with Tl p orbitals. The last two t sets also decompose to $3b_2$ and $1a_2$ orbitals that are only Ta−As bonding, and the same is true of $3a_1$. Therefore bonding of Tl to $TaAs_4$ originates largely with $1a_1$, $1b_2$, 1e, $2a_1$, $2b_2$, 2e, 3e, 4e. The progression of bonding contributions from As s and Tl s through σ p−p to π can be followed from the overlap populations per atom pair in Table 4.

The topologies of the four e MOs sketched in Chart 1 illustrate all of the important $\pi_\perp$, $\pi_\parallel$, and σ contributions in the ion, the last two classes referring to bonding orbitals lying within the $TlAs_2Ta$ planes. The nature of some significant σ components is seen around Ta too, the Ta p and d serving both purposes in 2e and 3e but being out of phase in 4e. (The drawings do not reflect relative coefficients.) The σ contributions from Tl s are particularly important in the lowest two a_1 and two b_2 levels and from As σ donations to Tl p, in 1e, $4b_2$, and $4a_1$. The Tl−As $\pi_\perp$ OP's are largest for 3e, while σ and $\pi_\parallel$ are most important in 2e. The importance of π bonding on the addition of Tl to $TaAs_4^{7-}$ is evident, but the shape of the ternary ion allows some significant σ contributions as well. The Tl p orbitals are pushed up (to 5e, 6e) on As donation into them. The large HOMO−LUMO gap calculated for $[TaAs_4Tl_2]^{5-}$, −2.4 eV, attests to both the stability of the ion suggested by

the syntheses and to the expected Zintl phase characteristic of $Rb_5TaAs_4Tl_2$.

Many transition-metal-based Zintl phases involve, like $TaAs_4Tl_2^{5-}$, tetrahedral bonding of p elements around the central metal of interest. With the usual σ- and π-bonding scheme, three nonbonding orbitals remain for additional electrons that might be localized on a reduced central metal, $MnAs_4^{9-}$ for example.[11] One can imagine that analogues of $TaAs_4Tl_2^{5-}$ with different elements might also be reducible, e.g., $TaSe_4Tl_2^{-}$.

Acknowledgment. We thank B. Huang, P. Maggard, and R. Henning for discussion on the structure and bonding and W. Straszheim for the EDS measurements.

Supporting Information Available: Two tables with additional crystallographic data and anisotropic displacement parameters (2 pages). Ordering information is given on any current masthead page.

IC9802395